Ocean and Coastal Research

ORIGINAL ARTICLE

http://doi.org/10.1590/2675-2824072.23148
ISSN 2675-2824

Contributions of rising mean river level of the Río de la Plata estuary on recorded changes in positive storm surges

M. Florencia de Azkue*[1,2], Enrique E. D'Onofrio[3]

[1] Departamento Oceanografía – Servicio de Hidrografía Naval (Av. Montes de Oca, 2124 – C1270ABV – Ciudad Autónoma de Buenos Aires – Argentina).
[2] Escuela de Ciencias del Mar – Facultad de la Armada – Universidad de La Defensa Nacional (Av. Antártida Argentina, 425 – C1104AAD — Ciudad Autónoma de Buenos Aires – Argentina).
[3] Facultad de Ingeniería – Universidad de Buenos Aires (Av. Paseo Colón, 850 – C1063ACV – Ciudad Autónoma de Buenos Aires – Argentina).

* Corresponding author: maria.azkue@defensa.gob.ar

ABSTRACT

A 117-year series of hourly-observed heights in the Río de la Plata estuary allows studying the recorded changes in positive storm surge (PSS) events spanning from 1905 to 2021, and calculate the annual mean river level (AMRL) trend. The analysis of PSS focuses on the trend of the annual number of events, the annual mean events duration, and the annual maximum PSS height. Seasonal analyses of these variables can also be conducted. This study aimed to ascertain any correlation between the rising AMRL and the evolution of PSS. Since AMRL increase is related to the effects of global warming, the observation series is divided into two periods based on the behavior of the curve of greenhouse gas emissions into the atmosphere. One period covers 1905 to 1962 and is characterized by a less pronounced curve slope, while the other period, 1965 to 2021, exhibits a drastically steeper curve slope. Moreover, two sets of data were obtained to calculate the PSS in two different scenarios for both periods: a hypothetical one, with no trend in AMRL, and a realistic one, maintaining the observed AMRL trend. The results show the acceleration trend of two of the analyzed variables, namely the annual number of events and the average duration of events, when transitioning from one period to the other (following the behavior observed in AMRL). However, the increase in AMRL could not be the only explanation of these accelerations. On the one hand, although the accelerations decrease when the hypothetical scenario is considered, they do not totally disappear. Moreover, the annual average duration of the events increases follows the realistic scenario when removing AMRL trend. On the other hand, the maximum height of PSS shows no trend in either period and remains unaffected comparing the two scenarios.

Keywords: Positive storm surges, Sudestadas, Annual mean river level, Climate change, Global warming

INTRODUCTION

Global climate change is leading to mean sea level rise, generating an increase in the frequency of coastal flooding (Vitousek et al., 2017). In addition, such rise and long-term changes in the magnitude, frequency, and trajectories of storms and positive storm surge (PSS) may alter the parameters of extreme water level distributions and the evolution of coastal hazards over time (Vitousek et al., 2017). In contrast to the large number of studies that have focused on global mean sea level changes, much less research has been devoted to determining the contribution of

Submitted: 11-Sep-2023
Approved: 03-May-2024

Associate Editor: Cesar Rocha

climate-driven changes in storm activity to extreme sea levels. Our understanding of how tides, PSS, and waves influence sea level extremes is only modest (Fox-Kemper et al., 2021). For their part, PSS are a major cause of coastal flooding and can have devastating social effects (Kron, 2013).

Río de la Plata (RdP) is a very large and shallow estuary with a NNW-SSE orientation shared by Argentina and Uruguay (Figure 1). On its shores and in its area of influence are the capitals of both countries, Buenos Aires and Montevideo, and numerous ports, resorts, and industrial centers. Formed by the confluence of the Paraná and Uruguay rivers, it drains the waters of the second largest basin of the subcontinent, after the Amazon River (Moreira and Simionato 2019). The RdP has a length of about 300 km, widening from 40 km at its upper end to 220 km at its mouth into the Atlantic Ocean, while the estuarine surface area is 35,000 km^2. The water level in the RdP is usually described by the combination of a semidiurnal microtidal regimen with diurnal inequalities (D'Onofrio et al., 2012) and its wind-driven circulation (Simionato et al., 2004, 2006). It is located in one of the most cyclogenic regions of the Southern Hemisphere (Gan and Rao, 1991) due to atmospheric waves moving along the subtropical latitudes of the South Pacific and South American regions. Anticyclonic cells that detach from the South Pacific high-pressure center and travel east-northeastward lead to the development of strong southeasterly winds in lower layers of the atmosphere that can exceed 25 ms^{-1} during extreme events (D'Onofrio et al., 1999). These storms, known as *sudestadas*, produce PSS and flooding in the upper estuary (D'Onofrio et al., 1999; Santoro et al., 2013; Dinápoli et al., 2017), although they can also be produced by other meteorological conditions that lead to strong and/or persistent easterly and southeasterly winds (Escobar et al., 2004). *Sudestadas* are associated with a circulation variability mode that prevails when the wind exhibits a dominant component aligned along the estuary axis, characterized by a distinct pattern of significant water level increase at the upper part of the estuary (Simionato et al., 2004, 2006). The wind action not only raises the river level but also generates more pressure at the discharge of the storm drains and streams that cross the city draining into the RdP estuary. This blocks the runoff of accumulated water in the city, causing flooding not only in shoreline areas but also in the valleys of these streams, where its sinkholes are located (Nabel et al., 2008). PSS events can last from one to three days, but longer duration cases have been recorded (Moreira et al., 2014). In fact, our analysis in this study revealed an extreme case lasting approximately 175 hours during 1976.

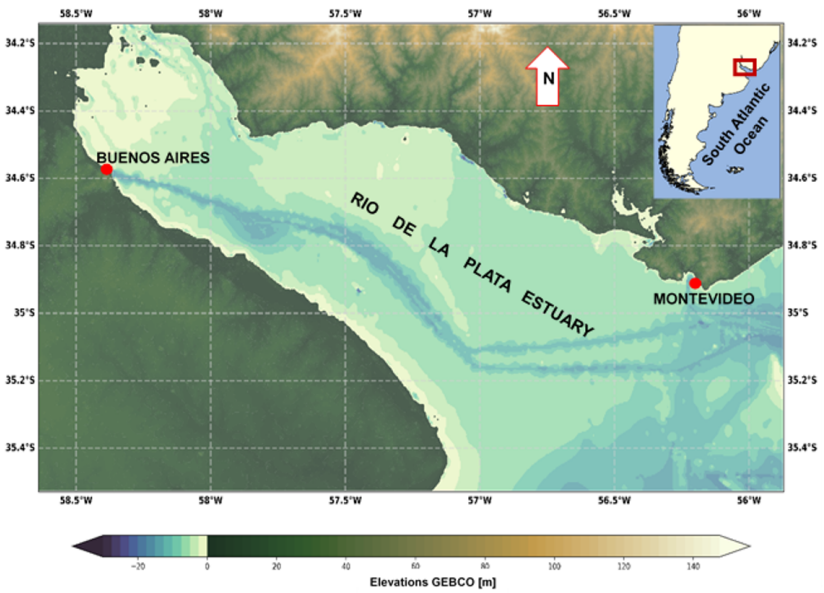

Figure 1. Location and bathymetry of the Río de la Plata estuary.

Similar to the ongoing trends observed in oceans worldwide, Río de la Plata (RdP) is undergoing a rise in its mean level attributed to global warming (e.g., Dennis et al., 1995, Santamarina-Aguilar et al., 2017; Piecuch, 2023), aligning with the South Atlantic Sea level pattern (Frederikse et al., 2021). Furthermore, there is an observed increase in the frequency and duration of *sudestadas*, seemingly linked to the relative rise in mean water level (D'Onofrio et al., 2008). Thus, these two combined effects lead to increased vulnerability of the coastal zone to flooding (Re and Menéndez, 2006).

Strong interactions can occur between tide, storm surge, waves, sea level rise, and flooding; nevertheless, the importance of each interaction mechanism is very heterogeneous depending on the location considered (Idier et al., 2019). In that sense, one can consider that there could be an interaction between PSS events and mean water level, as the PSS develop above this level. In this context, certain studies have demonstrated that the interaction between storm surge and sea level rise can be either linear or nonlinear (Zhang et al., 2012; De Dominicis et al., 2020). Therefore, in this work, we propose to analyze whether the increase of the annual mean river level (AMRL) contributes to the registered changes in PSS in the estuary of the RdP. For this purpose, we examined the evolution of the PSS in Buenos Aires, a location of the estuary that boasts a 117-year series of hourly heights, considering the contribution of the change of the AMRL in one case, and without considering it in another. Furthermore, as the rise in AMRL is associated with the impacts of global warming, we divided the observation series into two periods (1905-1962 and 1965-2021) based on the behavior of the curve of greenhouse gas emissions into the atmosphere. The curve during the first period is characterized by a less pronounced slope, while the second period exhibits a markedly steeper slope (e.g., Stoddard et al., 2021).

METHODS

Data

The baseline data used in this work to perform the PSS analyses correspond to the hourly heights of the RdP estuary in the period from 1905 to 2021. The height observations were performed with two different tide gauges. The first gauge was operated by the Ministry of Public Works and located at the mouth of the Riachuelo River—Semáforo del Riachuelo—from 1905 and 1959. The second gauge was operated by the Naval Hydrographic Service in the neighborhood of Palermo—Club de Pescadores, Palermo station—, 9 km north of the Riachuelo River, from 1957 and 2021. Thus, there are three years of overlapping data between both records (1957-1959). The coastline between the two stations does not show morphological differences and the tide observed at both stations has similar characteristics, making them comparable (D'Onofrio et al., 2008). The levels of both tide gauges are referenced to the zero or datum of the Riachuelo River, which is 0.531 m below the zero of the National Geographic Institute.

The zero of the Riachuelo River was established practically coincident with the level of the lowest astronomical low tides (Dirección Nacional de Control de Puertos y Vías Navegables, 2022). The final series of heights, from 1905 to 2021, covers 117 years, with a missing data interval from 1963 to 1964.

AMRL and linear trend

To obtain the AMRL and its linear trend, the series of observations is divided into two subsets of data. The first subset corresponds to the observations from 1905 to 1962, and the second to those from 1965 to 2021 (the periods are denoted as P1 and P2, respectively). This distinction is based on changes observed in the curve of greenhouse gas emissions into the atmosphere related to the effects of global warming. As a consequence of such warming there has been an increase in the mean RdP level, which has accelerated, as in the rest of the global ocean, around 1960 (e.g., de Azkue and Fiore, 2021). For the two-height series, the annual mean levels were estimated by considering the arithmetic mean of all the observations corresponding to each year and by employing a Savitzky-Golay filter (Savitzky and Golay, 1964) with a polynomial order of 3 and a window size of 31 on annual data. In the computed values of the annual arithmetic mean of

hourly tide heights, various contributions were anticipated, stemming from astronomical tidal cycles exceeding one year, including the Metonic cycle of approximately 19 years. Haight et al. (2011) determined that in the region spanning from the North Sea to the central Baltic Sea, the highest astronomical tides manifest at intervals of 74.4 and 55.8 years, which are multiples of modulation cycles lasting 18.6 years. Lopez (2023), focusing on the Patagonian shelf, established that, in most instances, a 30-year period is adequate for the extreme astronomical tide values to converge. This insight guided the choice of a 31-year window width for the Savitzky-Golay filter. Simultaneously, a polynomial order of 3 was selected based on empirical evidence showing minimal distortion in the peaks or fine details of the original data. A comprehensive elucidation of the Savitzky-Golay filter can be found in Luo et al. (2005), with applications in oceanography and hydrography detailed by Lycourghiotis and Kontini (2012) and Alsaaq et al. (2016). To facilitate result comparison, the predicted astronomical tide was subtracted from the hourly height series, and subsequently, the arithmetic mean was calculated annually. This process yields new series of annual mean levels, which are then compared with those calculated from the filtering. The trend of the filtered series was obtained by fitting to a least squares line and the Pearson coefficient (r) was estimated.

Astronomical tide and residual series

To calculate the PSS events, it is necessary to have a series of residuals consisting of the difference between the observed height and the astronomical tide. Thus, harmonic least squares analyses are performed following Equation 1

$$h(t) = Z_0 + \Delta Z\ .\ t + \sum_{j=1}^{n} H_j\ f_j\ cos\ ((V+u)_j - g_j)$$

Equation (1)

where subindex j refers to each tidal component, t corresponds to the time of each observation, h is the observed height, Z_0 is the mean river level of the period, ΔZ is the variation of the mean level, H is the amplitude of the components, f is the nodal factor, (v+u) is the equilibrium argument, and g corresponds to the modified epoch.

This methodology considers the possible linear variations of the mean sea level by adding the straight line $Z_0 + \Delta Z\ .\ t$ and obtaining the harmonic constants directly (D'Onofrio et al., 2016). The equilibrium arguments and nodal factors were estimated considering the time scales presented by Cartwright (1985). The estimation of error-components included in the harmonic analyses was performed from the variance-covariance matrix, which arises from the methodology used in the harmonic analyses. A total of 134 constituents were included in the harmonic analysis, allowing a wide range of frequencies to be considered.

Although the harmonic constants are so called since their value does not change over time, factors such as changes in mean sea level, bathymetry, river discharge, or thermohaline can alter the value of these constants (e.g., Santamaria-Aguilar et al., 2017, Luz Clara et al., 2014). In order to consider these possible changes and address the Metonic cycle, harmonic analyses were performed to the observations, dividing them into five periods of 19 years (1905–1923, 1924–1942, 1965–1983, 1984–2002, 2003–2021) and one of 20 years (1943–1962). In other words, six sets of harmonic constants were obtained.

Likewise, astronomical tide predictions were estimated in two different ways for each period (P1 and P2). The first, considering i) all the harmonic constants obtained in the 19/20-year periods, ii) the mean river level of the period, and iii) the linear variation of the AMRL. The second followed the same criteria as the first, except that it did not consider the AMRL trend.

From these four series of predictions, we obtained the series of residuals to estimate PSS events, subtracting from the observations the series of predictions in each case. The four series of residuals include:

$$Residuals_1 = observations\ (1905-1962) - astronomical\ tide\ (19\ years\ harmonic\ constants) - mean\ river\ level\ (1905-1962) - AMRL\ trend\ (1905-1962)$$

Equation (2)

$$Residuals_2 = observations\ (1905 - 1962) - astronomical\ tide\ (19\ years\ harmonic\ constants) - mean\ river\ level\ (1905 - 1962)$$

Equation (3)

$$Residuals_3 = observations\ (1965 - 2021) - astronomical\ tide\ (19\ years\ harmonic\ constants) - mean\ river\ level\ (1965 - 2021) - AMLR\ trend\ (1965 - 2021)$$

Equation (4)

$$Residuals_4 = observations\ (1965 - 2021) - astronomical\ tide\ (19\ years\ harmonic\ constants) - mean\ river\ level\ (1965 - 2021)$$

Equation (5)

Thus, the series Residuals$_1$ (R1) and Residuals$_3$ (R3) have the AMRL trend removed and are part of a hypothetical scenario, while the other two series, Residuals$_2$ (R2) and Residuals$_4$ (R4) belong to a realistic scenario since they maintain the contribution of the AMRL trend.

Determination of PSS events

To obtain the heights corresponding to the PSS events, we started from the series of estimated residuals, as described in the previous section. Not all obtained residuals correspond to PSS events. The events must satisfy the following criteria: i) they must never fall below 0.30 m, ii) the highest residual of the event must be larger than or equal to 1.60 m, and iii) the events must last at least six hours. The value of 0.30 m set as the threshold for PSS events was adopted because, under calm meteorological conditions, there may be a difference between the observed heights and the astronomical tide of the order of ±0.10 m. Thus, to ensure that the chosen residuals correspond to PSS events, the threshold value adopted is three times the above-mentioned difference. Regarding the value of 1.60 m, it was adopted since, when combined with a tidal height close to mean river level (approximately 0.79 m above the zero of the Riachuelo River) during a semi-diurnal rising tide, it leads to levels that can approach the warning levels of the City of Buenos Aires and its surroundings (D'Onofrio et al., 2008). In addition, to ensure that it is really a PSS event and not a recorded anomalous height, a minimum duration of at least six hours was chosen. Once the events were determined, the annual trends of the time series of the following variables were estimated: annual number of events, mean annual duration, annual maximum observed height, and annual maximum PSS height. For this purpose, as in the estimation of the AMRL trend, a Savitzky-Golay filter (Savitzky and Golay, 1964) was first applied with a polynomial order of 3 and a window size of 31 on annual data. The smoothing of the data intends to identify long-term trends more clearly, without the interference of other present fluctuations. Then, the trend was obtained to a least squares line fitting for the periods 1905–1962 and 1965–2021, and the Pearson coefficient (r) was also estimated. These estimations were performed with the residual series R2 and R4 (which contain the trend of the AMRL) and with the residual series R1 and R3 from which the trend was removed. Moreover, to enhance the completeness of the analysis, a seasonal study of the events for both periods in the realistic scenario was conducted.

RESULTS

Annual trends

The results derived from the annual river level series, obtained by applying the Savitzky-Golay filter and by subtracting predictions, exhibited similarity, with differences on the order of a millimeter. We opted to retain the filtered series for trend analysis.

The annual marches and trends of AMRL, maximum observed height, number of PSS events, mean annual duration of events, and maximum PSS height were plotted in Figures 2,3,4,5 and 6, respectively. On the left of each Figure, the period 1905–1962 (P1) is represented, and on the right side the period 1965–2021 (P2). The results of the number of PSS events, mean duration, and maximum PSS height presented in Figures 4, 5,

and 6 were obtained from the R2 and R4 residual series corresponding to the realistic scenario, in which the AMRL trend was maintained. Figures 7, 8, and 9 show the results of these three variables for the hypothetical scenario, in which the AMRL trend was removed, obtaining the results from the R1 and R3 residual series. Figure 2 shows how the AMRL trend doubles its value at P2 (B) compared with P1 (A), going from 0.0011 m yr^{-1} to 0.0023 m yr^{-1}. The trend of the maximum observed height (Figure 3) not only increased from P1 (A) to P2 (B), but also reversed its sign. It changed from a negative trend (−0.0015 m yr^{-1}) in P1 to an increasing trend in P2 with a value of 0.0027 m yr^{-1}. Regarding the trend of the annual number of PSS events (Figure 4), as we moved from one period to the other, we noted that its value increased by an order of magnitude, being 0.0117 events yr^{-1} in P1 and 0.1435 events yr^{-1} in P2. Figure 5 shows, for the mean duration of the events, how the trend also increased from one period to the other and reversed the sign as did the trend of the maximum observed height, being −0.0327 h yr^{-1} in P1 and 0.018 h yr^{-1} in P2. Regarding the maximum PSS height (Figure 6), it showed no trend in both periods (we highlight the low values of the Pearson coefficient). When observing the number of annual events in the hypothetical scenario with no change in the mean river level trend (Figure 7), we noted that this trend preserved the same behavior as in the realistic scenario (Figure 4), in which the value increased by an order of magnitude when going from P1 to P2. In addition, the value between scenarios for the same period barely decreases (from 0.0117 events yr^{-1} with R2 to 0.0115 events yr^{-1} with R1, and from 0.1435 events yr^{-1} events with R4 to 0.1221 events yr^{-1} with R3). Figure 9 shows the maximum PSS height, which remained trendless between periods, as for the realistic scenario (Figure 6). The trend of the mean duration in the hypothetical scenario (Figure 8) increased and reversed the sign when going from P1 to P2, with values of −0.0353 h yr^{-1} and 0.0245 h yr^{-1}, respectively. However, the values corresponding to P2 are lower than those from the realistic scenario, in which the increase of the mean river level was retained in residuals (Figure 5).

In Figure 10, the R3 and R4 residual series on certain days in 2015 were plotted to observe their patterns and make comparisons. The theoretical initial height and the theoretical height to be exceeded by the maximum PSS were also indicated with horizontal blue lines. Apart from the noticeable lag in certain segments of the curves, it is evident that the peaks of the first two storms exceeded the theoretical threshold in the case of the R4 residuals but not in the case of R3. Consequently, these two events were considered as PSS events in the realistic scenario but not in the hypothetical one. However, the third surge documented in the record was classified as a PSS event in both scenarios, as both residual series satisfy the criterion of exceeding the height of 1.6 m.

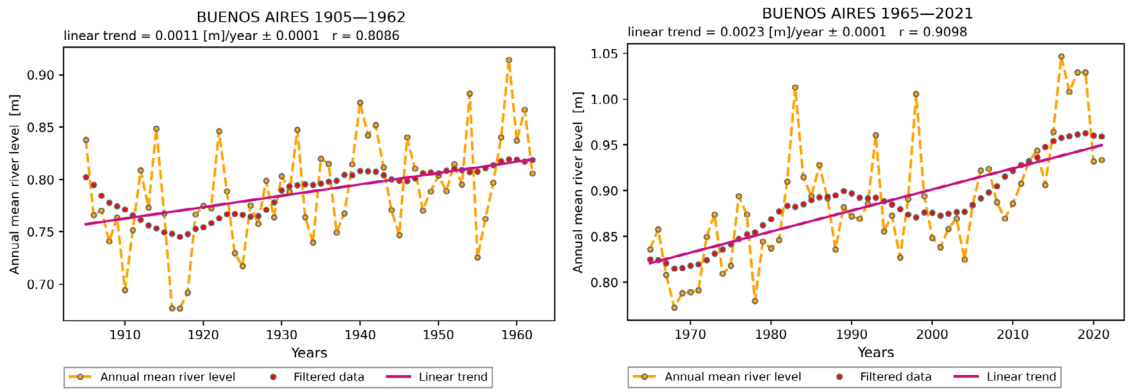

Figure 2. A) AMRL trend during P1 period (from 1905 to 1962) and B) AMRL trend during P2 period (from 1965 to 2021).

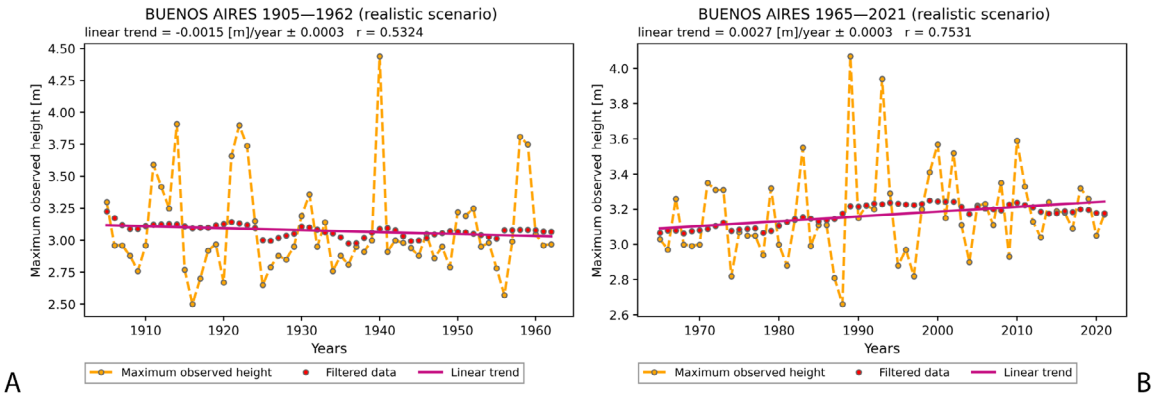

Figure 3. Maximum observed height trend in a realistic scenario (considering the AMRL trend). A) During the P1 period (from 1905 to 1962). B) During the P2 period (from 1965 to 2021).

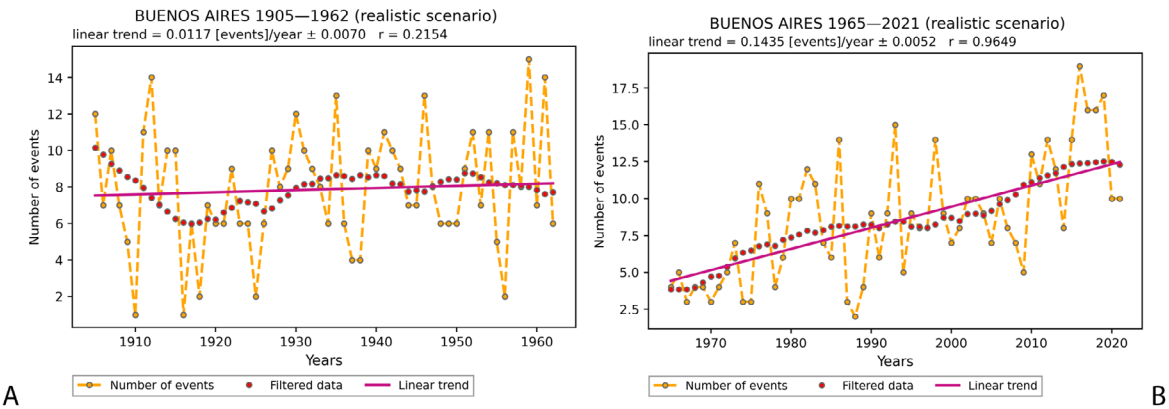

Figure 4. Number of PSS events in a realistic scenario (considering AMRL trend). A) During P1 period (from 1905 to 1962). B) During P2 period (from 1965 to 2021).

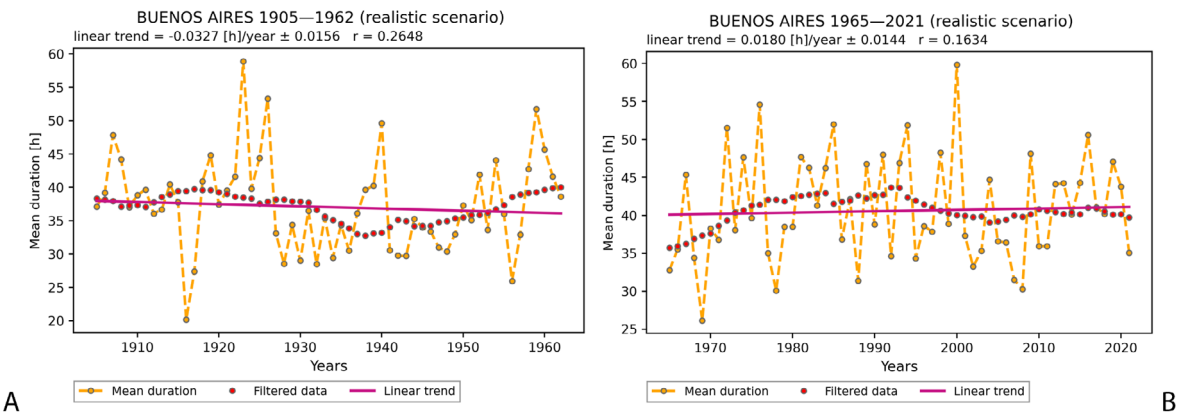

Figure 5. PSS events mean duration trend in a realistic scenario (considering the AMRL trend). A) During the P1 period (from 1905 to 1962). B) During the P2 period (from 1965 to 2021).

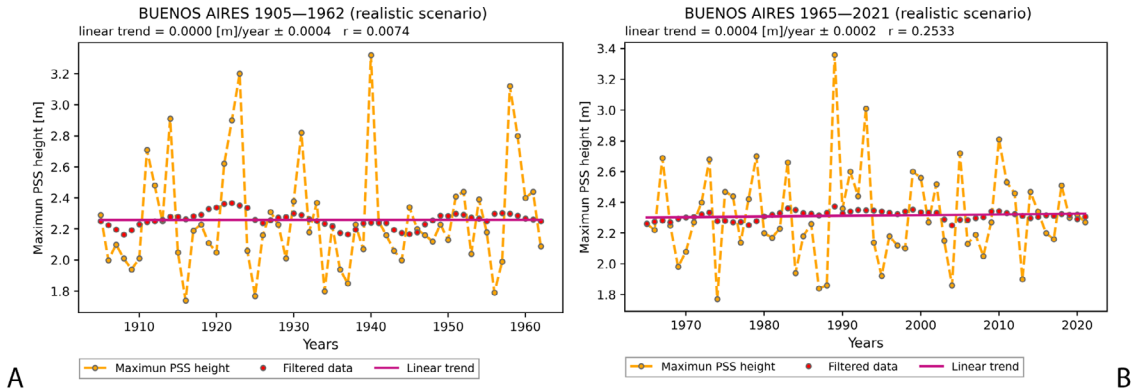

Figure 6. Maximum PSS height trend in a realistic scenario (considering the AMRL trend). A) During the P1 period (from 1905 to 1962). B) During the P2 period (from 1965 to 2021).

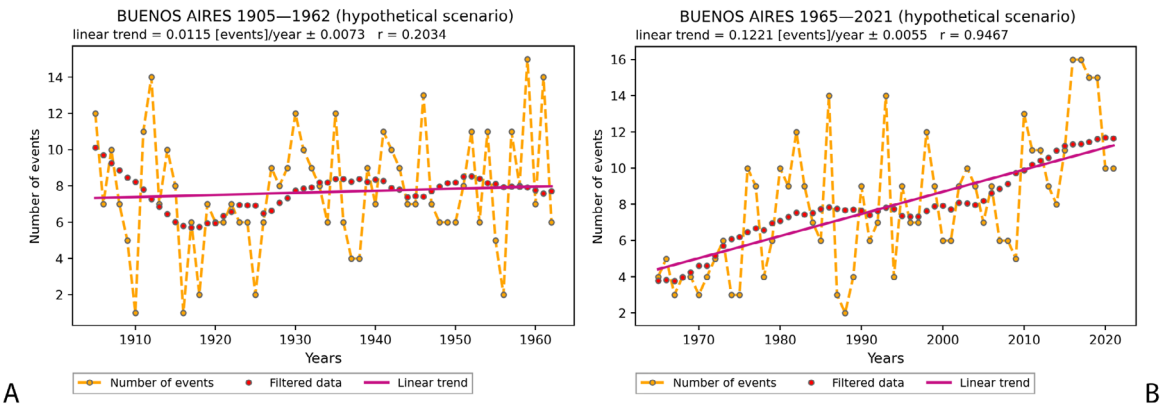

Figure 7. Number of PSS events trend in a hypothetical scenario (not considering AMRL trend). A) During P1 period (from 1905 to 1962). B) During P2 period (from 1965 to 2021).

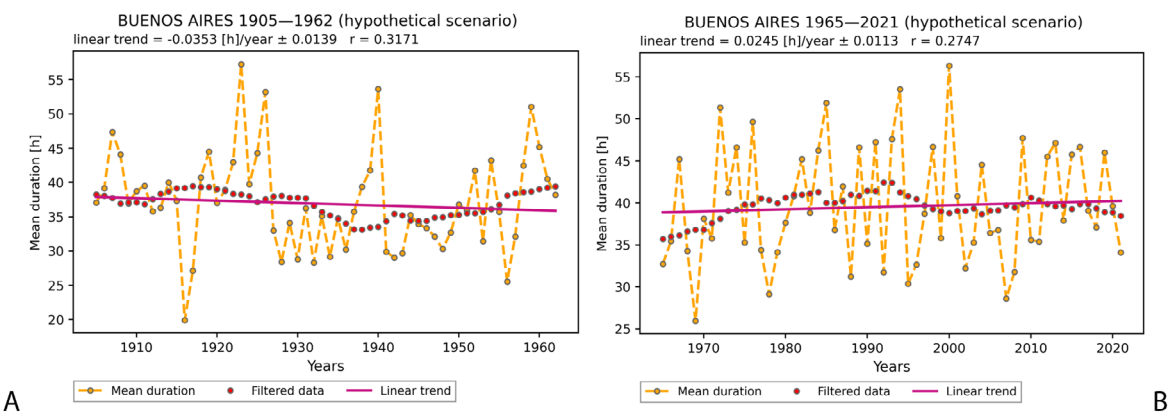

Figure 8. PSS events mean duration trend in a hypothetical scenario (not considering AMRL trend). A) During the P1 period (from 1905 to 1962). B) During the P2 period (from 1965 to 2021).

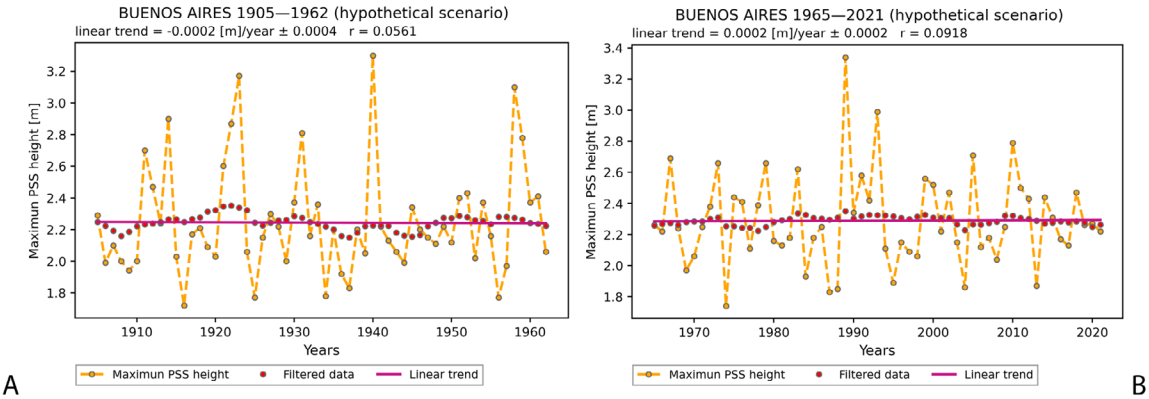

Figure 9. Maximum PSS height trend in a hypothetical scenario (not considering AMRL trend). A) During the P1 period (from 1905 to 1962). B) During the P2 period (from 1965 to 2021).

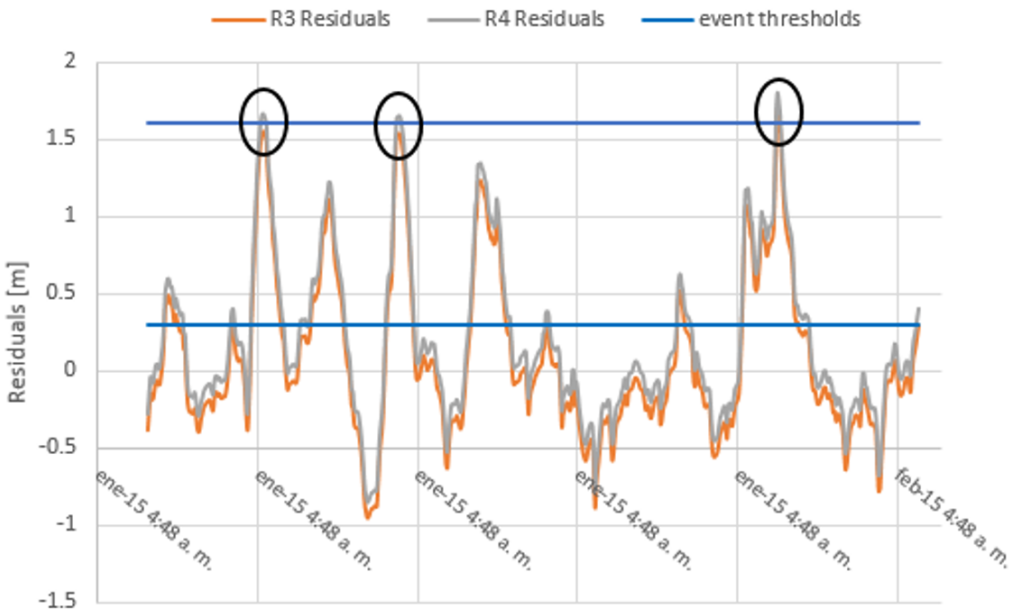

Figure 10. Example of the observed behavior from R3 (hypothetical scenario) and R4 (realistic scenario) residuals series on certain days in 2015. Horizontal blue lines mark the theoretical initial height and the theoretical height to be exceeded by the maximum of the PSS.

Seasonal analysis

Figure 11 shows the distribution of the number of events by season for the periods P1 and P2 calculated with the residual series R2 and R4 (realistic scenario). For both periods, it can be noted that summer held the highest number of events, followed by spring, autumn and, finally, winter, with the lowest number. This result is opposite to that of Nabel et al. (2008), who found that the highest number of events occurred in winter. The difference may be due to the criteria used to determine the events and time period considered for both analyses. However, the results of this work are consistent with the distributions presented by Escobar et al. (2004), in which a higher frequency of *sudestadas* was observed both in summer and spring. It can also be observed that the increase in the number of

events in the P2 period when compared to P1 occurred mainly in the spring and winter months. For summer and autumn, the number of events remained practically constant between periods. Figure 12 shows the seasonal distribution of the number of events obtained with the R2 and R4 residual series over the years. The gray colors correspond to seasons without events (due to the establishment of a threshold for the events, in this case 1.60 m), whereas the blue color corresponds to the years 1963 and 1964, in which no information is available. It is easy to identify summer as the modal season, with a noticeable increase (darker colors) in the number of events occurring in the springs of the most recent years of the record and in a short period after 1980.

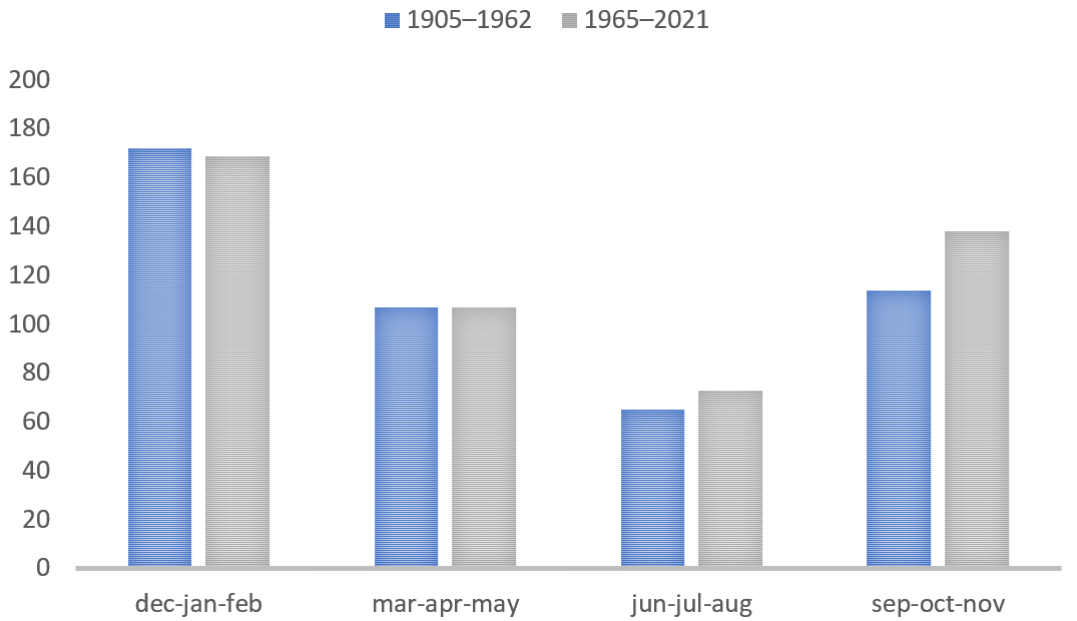

Figure 11. Number of PSS events per season of the year, for the P1 (blue color bars) and P2 (grey color bars) periods calculated with the R2 and R4 residual series (realistic scenario).

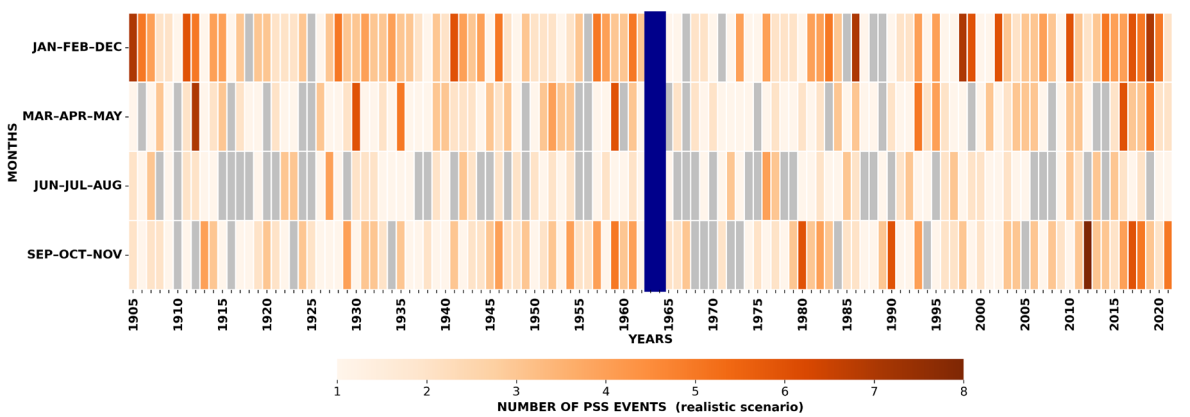

Figure 12. Seasonal distribution as a function of years of PSS events obtained with R2 and R4 residual series (realistic scenario).

Both the maximum observed height and the maximum PSS show, seasonally, a similar behavior, so the results are shown for the maximum PSS only during the two periods analyzed, obtained from the R2 and R4 residual series (Figure 13). Here, it can be seen that the maximum PSS corresponds

to a spring of period P2 with a value of 3.36 m, and that summers have the lowest maximum height, despite being the season that records the most events in both periods. It is also observed that only in the case of spring and summer for the period P2 the maximum PSS exceeds that of the period P1. There is not a wide difference between seasons. Figure 14 shows the annual distribution of these maximum PSS heights (for residuals R2 and R4) for each season and assigns the spring of 1989 as the maximum event for its height, followed by the event recorded in the fall of 1940 (historical record of maximum observed height). Both events are the highest for the period P2 and P1, respectively. The same figure shows that, from 2008 onwards, the spring records the highest values in a more persistent manner than in previous years. This behavior is the same when the seasonal distribution is analyzed with the R1 and R3 residuals to which the trend of the mean river level was removed (hypothetical scenario).

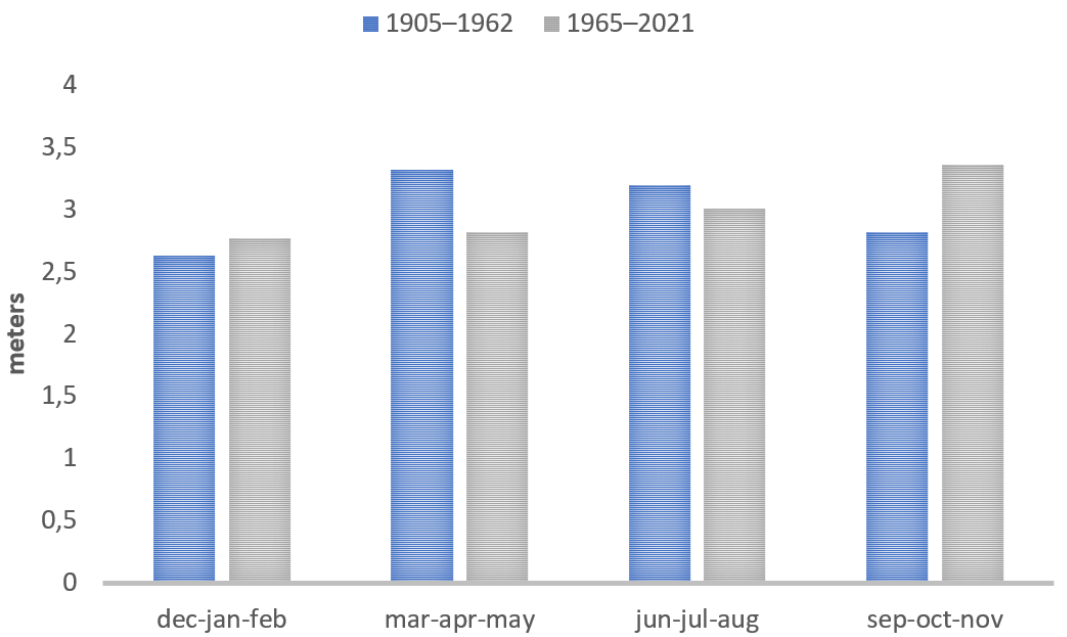

Figure 13. Seasonal distribution of the maximum PSS for the P1 (blue color bars) and P2 (grey color bars) periods obtained from R2 and R4 residuals series (realistic scenario).

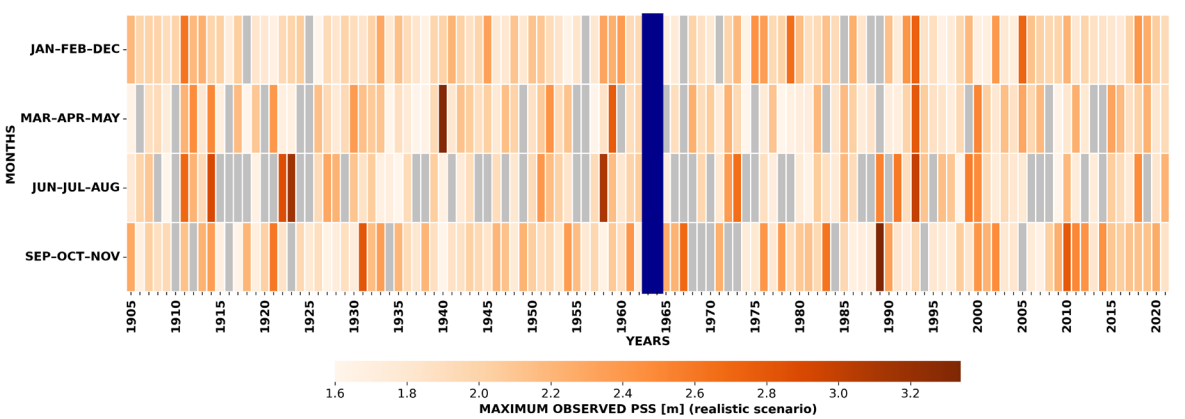

Figure 14. Seasonal distribution as a function of years considering the maximum PSS obtained from R2 and R4 residual series (realistic scenario).

Figure 15 shows the seasonal distribution of the mean duration of PSS events obtained from the residuals R2 and R4 belonging to the realistic scenario for the two periods analyzed. The mean duration is higher in the summers, autumns, and springs of the second period compared to the first. The modal interval is that corresponding to winter in both periods, although it is the season with the lowest number of events, as seen previously (Figure 11). It is also found that, although the longest events occur during winters—considering the entire 117-year period (Figure 15)— this behavior shifts to spring events in recent years (not shown). In other words, not only are most PSS events taking place in recent springs, but these events are also lasting longer.

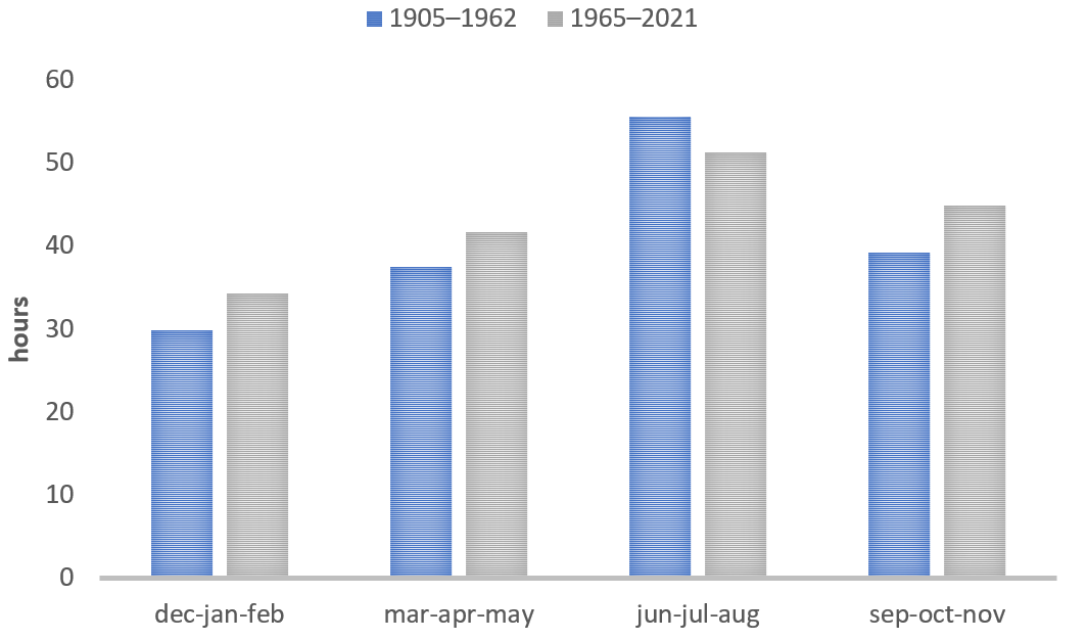

Figure 15. Seasonal distribution of the mean duration of PSS events for the P1 (blue color bars) and P2 (grey color bars) periods obtained from the R2 and R4 residuals series (realistic scenario).

The results obtained from the seasonal analysis corresponding to the realistic scenario described in the previous paragraphs are analogous to those of the residual series calculated in a hypothetical scenario, in terms of the observed behavior.

DISCUSSION

The analysis conducted comparing the realistic scenario (the one that considers the AMRL trend) and the hypothetical scenario (the one that does not consider this trend) allows us to state that some of the changes found in the PSS cannot be solely and directly attributed to the increase in the AMRL. Some behaviors are found to support this. In the case of the trend of the annual number of events, we found that, when going from P1 to P2, it increased by an order of magnitude in the realistic scenario, while the trend of the AMRL doubled. In addition, in the hypothetical scenario, the increase of one order of magnitude in the passage from P1 to P2 was maintained, so it cannot be the AMRL variation that models these changes, as this variation is not considered in the latter scenario. Thus, this increase, which occurs mainly during the springs of recent years and to a lesser extent in winters, could be due to changes in atmospheric circulation (Laignel et al., 2023) and the local and regional wind pattern, as well as changes in the discharge of rivers that flow into the estuary of the Río de la Plata and modify the AMRL (Piecuch, 2023).

The lack of trend in the maximum annual PSS height, both between periods and scenarios, also shows that this variable is not directly affected by the increase in AMRL. In this case, interactions

with the astronomical tide may model the observed behavior. Sea level rise could slightly dampen tidal heights due to nonlinear interactions between tides and PSS (Wood et al., 2022). Tidal cycles, such as the 18.61-year cycle caused by the precession of the Moon's orbit around the Earth, can influence extreme water levels (Haigh et al., 2011; Peng et al., 2019). These variations were included when performing harmonic analysis over periods of 19/20 years. Thus, in the context of sea-level rise, storm surges experience an influence from reduced bottom friction, leading to an augmentation of storm surges (Idier et al., 2019). Nevertheless, as demonstrated by Arns et al. (2017) in the North Sea, the reduction in bottom friction seems to be offset by the diminished effectiveness of surface wind stress. In essence, the identical wind forcing is less efficient in displacing water and results in a smaller surge when the water depth is larger. Thus, these combined effects could explain the results obtained in the annual maximum height of PSS too.

Regarding the trend of the mean annual duration of PSS events, it is interesting to note that it presented higher values in the hypothetical scenario than in the realistic one, showing a behavior opposite to that of the AMRL trend. Moreover, this trend is determined by the behavior of events in winter since it is the only season of the year in which the average duration is shorter during P2 period. Notably, however, the Pearson coefficient values for this variable have yielded statistically insignificant results.

Finally, as expected, the seasonal analysis of the considered variables yielded higher values for the series of residuals representing the realistic scenario. However, as noted, the mean duration of the PSS deviates from this behavior.

CONCLUSION

The effects of climate change are noticeable, manifesting in changes in the different forcings of the PSS in the Río de la Plata estuary and in the processes that interact with them. The impacts of the increase in the AMRL on the evolution of the PSS cannot be omitted, although it has been shown that it is not the only or the most important cause affecting them. There is also a meteorological component that models them and explains some of the observed variations throughout the study period. The role of the atmosphere is playing a crucial role, as well as its fluctuations. Thus, complementing this work with studies on local and regional atmospheric circulation becomes a priority.

Beyond helping to understand the causes that originate the observed changes in the PSS—and detecting those changes—, this work may constitute a valuable tool when planning sustainable infrastructure works and sustainable non-structural measures in the City of Buenos Aires. We believe that it will aid in addressing the historical problem of flooding caused by PSS, as it monitors its forcing mechanisms.

ACKNOWLEDGMENTS

This work was supported by the project B-ESCM-0009/22 (Escuela de Ciencias del Mar, Facultad de la Armada, Universidad de la Defensa Nacional).

We would like to express our gratitude to the reviewers for their contribution in enriching and improving our work.

AUTHOR CONTRIBUTIONS

M.F.d.A.: Conceptualization; Investigation; Methodology; Resources; Writing – original draft; Writing – review & editing.

E.E.D.: Conceptualization; Investigation; Methodology; Software; Formal Analysis; Supervision; Writing – review & editing.

REFERENCES

Alsaaq, F., Kuhn, M., El-Mowafy, A. & Kennedy, P. 2016. *Filtering methods to extract the tide height from Global Navigation Satellite Systems (GNSS) signals for Hydrographic applications*. In *Proceedings HYDRO 2016*. Rostock-Warnemünde: DHYG. Available from: http://hdl.handle.net/20.500.11937/75923. Access date: Dec. 21, 2023

Arns A., Wahl, T., Dangendorf, S., Jensen, & Pattiaratchi, C. 2017. Sea-level rise induced amplification of coastal protection design heights. *Scientific Report*, 7, 40171. DOI: https://doi.org/10.1038/srep40171

Cartwright, D. E. 1985. Tidal prediction and modern time scales. *International Hydrographic Review,* LXII(1), 127–138.

D'onofrio, E., Fiore, M.M.E. & Romero, S. 1999. Return periods of extreme water levels estimated for some vulnerable areas of Buenos Aires. *Continental Shelf Research*, 19, 1681–1693.

D'onofrio, E. E., Fiore, M. E. & Pousa, J. L. 2008. Changes in the regime of storm surges in Buenos Aires, Argentina. *Journal of Coastal Research,* 24(1A), 260–265.

D'onofrio, E. E., Oreiro, F. A., Grismeyer, W. H., & Fiore, M. M. E. 2016. Predicciones precisas de marea astronómica calculadas a partir de altimetría satelital y observaciones costeras para la zona de Isla Grande de Tierra del Fuego, Islas de los Estados y Canal de Beagle. *GEOACTA,* 40(2), 60–75.

D'onofrio, E. E., Oreiro, F. & Fiore, M. E. 2012. Simplified empirical astronomical tide model: an application for the Río de la Plata estuary. *Computational Geosciences,* 44, 196–202. DOI: https://doi.org/10.1016/j.cageo.2011.09.019

De Azkue, M. F. & Fiore, M. M. E. 2021. Análisis de la tendencia relativa del nivel medio del Río de la Plata entre 1905 y 2020. *Terra Mundus*, 8(1), 1-12.

De Dominicis, M., Wolf, J., Jevrejeva, S., Zheng, P. & Hu, Z. 2020. Future interactions between sea level rise, tides, and storm surges in the world's largest urban area. *Geophysical Research Letters*, 47(4), e2020GL087002.

Dennis, K.C., Schnack, E. J., Mouzo, F. H. & Orona, C. R. 1995. Sea level rise and Argentina: potential impacts and consequences. *Journal of Coastal Research*, 14, 205–223.

Dinápoli, M.G., Simionato, C.G. & Moreira, D. 2017. Model sensitivity for the prediction of extreme sea level events at a wide and fast-flowing estuary: the case of the Río de la Plata. *Natural Hazards and Earth System Sciences Discussions*, preprint. DOI: https://doi.org/10.5194/nhess-2016-393

Dirección Nacional de Control de Puertos y Vías Navegables. 2022, 19 de octubre. *Boletín Fluvial*. Buenos Aires. Available from: https://www.argentina.gob.ar/sites/default/files/2018/04/boletin_fluvial_42_22.pdf, accessed on 21/12/2023

Escobar, G., Vargas, W. & Bischoff, S. 2004. Wind tides in the Rio de la Plata estuary: meteorological conditions. *International Journal of Climatology: A Journal of the Royal Meteorological Society*, 24(9), 1159–1169.

Fox-Kemper, B., Hewitt, H. T., Xiao, C., Aðalgeirsdóttir, G., Drijfhout, S. S., Edwards, T. L., Golledge, N. R., Hemer, M., Kopp, R. E., Krinner, G., Mix, A., Notz, D., Nowicki, S., Nurhati, I. S., Ruiz, L., Sallée, J.-B., Slangen, A. B. A. & Yu, Y. 2021. Ocean, cryosphere and sea level change. *In*: Masson-Delmotte, V., Zhai, Pirani A., Connors. S. L., Péan, C., Berger, S., Caud, N., Chen, Y., Goldfarb, L., Gomis, M. I., Huang, M., Leitzell, K., Lonnoy, E., Matthews, J. B. R., Maycock, T. K., Waterfeld, T., Yelekçi, O., Yu, R. & Zhou, B. (eds). *Climate Change 2021: The Physical Science Basis. Contribution of Working Group I to the Sixth Assessment Report of the Intergovernmental Panel on Climate Change*. (pp. 1211–1362). Cambridge: Cambridge University Press. DOI: https://doi.org/10.1017/9781009157896.011

Frederikse, T., Adhikari, S., Daley, T. J., Dangendorf, S., Gehrels, R., Landerer, F., Marcos, M., Newton, T. L., Rush, G., Slangen, A. B. A., & Wöppelmann, G. 2021. Constraining 20th-century sea level rise in the South Atlantic Ocean. *Journal of Geophysical Research-Ocean*s, 126(3), e2020JC016970. DOI: https://doi.org/10.1029/2020JC016970.

Gan, A. P. & Rao, B. V. 1991. Surface cyclogenesis over South America. *Monthly Weather Review*, 119, 1293–1302. DOI: https://doi.org/10.1175/1520-0493(1991)119<1293:SCOSA>2.0.CO;2

Haigh, I. D., Eliot, M. & Pattiaratchi, C. 2011. Global influences of the 18.61 year nodal cycle and 8.85 year cycle of lunar perigee on high tidal levels. *Journal of Geophysical Research, Oceans*, 116(C6). DOI: https://doi.org/10.1029/2010JC006645

Idier, D., Bertin, X., Thompson, P. & Pickering, M. D. 2019. Interactions between mean sea level, tide, surge, waves and flooding: mechanisms and contributions to sea level variations at the coast. *Survey Geophysics,* 40, 1603– 1630. DOI: https://doi.org/10.1007/s10712-019-09549-5

Kron, W. 2013. Coasts: the high-risk areas of the world. *Natural Hazards*, 66, 1363–1382. DOI: https://doi.org/10.1007/s11069-012-0215-4

Laignel, B., Vignudelli, S., Almar, R., Becker, M., Bentamy A., Beneviste, J., Birol, F., Frappart, F., Idier, D., Salameh, E., Passaro, M., Menende, M., Simard, M., Turki, E. I. & Verpoorter, C. 2023. Observation of the coastal areas, estuaries and deltas from space. *Surveys in Geophysics*, 44, 1309–1356. DOI: https://doi.org/10.1007/s10712-022-09757-6

Lycourghiotis, S. & Kontoni, D.-P. 2012. *Analyzing the Flood Risk in Mediterranean Coastal Areas with a New Methodology*. In: 5th International Conference from Scientific Computing to Computational Engineering, Athens (pp. 4-7).

Lopez, M. I. 2023. *Obtención de planos de reducción de sondajes en el Mar Argentino para cartas náuticas a partir de datos mareográficos y constantes armónicas del Centro de estudios Topográficos del Océano y la Hidrósfera* (Tesina de Licenciatura en Cartografía). Escuela de Ciencias del Mar, Facultad de la Armada, Universidad de la Defensa Nacional, Buenos Aires. Available from: https://cefadigital.edu.ar/handle/1847939/2447. Access date: Dec 21, 2023

Luo J., Ying K. & Bai J. 2005. Savitzky–Golay smoothing and differentiation filter for even number data. *Signal Processing*, 85(7), 1429–1434. DOI: https://doi.org/10.1016/j.sigpro.2005.02.002

Luz Clara, M., Simionato, C. G., D'onofrio, E., Fiore, M. & Moreira, D. 2014. Variability of tidal constants in the Río de la Plata estuary associated to the natural cycles of the runoff. *Estuarine, Coastal and Shelf Science*, 148, 85-96. DOI: https://doi.org/10.1016/j.ecss.2014.07.002

Moreira, D., Briche, E., Falco, M., Robledo, F. A., Murgida, A., Cad, M., Partucci, H.B., Gatti, I., Duville, M., Re, M., Lecertua, E., Kazimierski, L. D., Etala, P., Campetella, C., Ruiz, J., Vera, C., Saulo, A. C., Simionato, C. G., Saraceno, M., Clara, M. L., D'Onofrio, E., Dragani, W., Bertolotti, M., Saucedo, M. & Vidal, R. 2014. "Anticipando la Crecida". Tools for the contribution in risk and disaster management due o southeasterly winds and precipitation floods in "La Ribera" district, Buenos Aires province, Argentina. *In*: *Colloque international "Connaissance et compréhension des risques côtiers"* (pp. 244-251). Available from: https://www.researchgate.net/publication/271848012. Access date: Dec 21, 2023

Moreira, D. & Simionato, C.G. 2019. Modeling the suspended sediment transport in a very wide, shallow, and microtidal estuary, the Rıo de la Plata, Argentina. *Journal of Advances in Modeling Earth Systems*, 11(10), 3284–3304. DOI: https://doi.org/10.1029/2018MS001605

Nabel, P.E. Caretti, M. & Becerra Serial, R. 2008. Incidencia de aspectos naturales y antrópicos en los anegamientos de la ciudad de Buenos Aires. *Revista Museo Argentino de Ciencias Naturales*, 10(1), 37–53.

Peng, D., Hill, E. M., Meltzner, A. J. & Switzer, A. D. 2019. Tide gauge records show that the 18.61-year nodal tidal cycle can change high water levels by up to 30 cm. *Journal of Geophysical Research, Oceans*, 124(1), 736–749. DOI: https://doi.org/10.1029/2018JC014695

Piecuch, C. G. 2023. River effects on sea-level rise in the Río de la Plata estuary during the past century. *Ocean Science*, 19(1), 57–75. DOI: https://doi.org/10.5194/os-19-57-2023

Re, M. & Menéndez, A. N. 2006. Impacto del cambio climático en las costas del Río de la Plata. *Revista Internacional de Desastres Naturales, Accidentes e Infraestructura Civil*, 7(1), 25.

Santamaria-Aguilar, S., Schuerch, M., Vafeidis, A. & Carretero, S. C. 2017. Long-Term Trends and Variability of Water Levels and Tides in Buenos Aires and Mar del Plata, Argentina. *Frontiers in Marine Science: Coastal Ocean Processes,* 4. DOI: https://doi.org/10.3389/fmars.2017.00380

Santoro, P. E., Fossati, M. & Piedra-Cueva, I. 2013. Study of the meteorological tide in the Río de la Plata. *Continental Shelf Research*, 60, 51–63.

Savitzky, A. & Golay, M. J. E. 1964. Smoothing and differentiation of data by simplified least-squares procedures. *Analytical Chemistry*, 36(8), 1627–1639. DOI: https://doi.org/10.1021/ac60214a047

Simionato, C.G., Dragani, W.C., Meccia, V. L & Nuñez, M. N. 2004. A numerical study of the barotropic circulation of the Rio de la Plata Estuary: sensitivity to bathymetry, the earth's rotation and low frequency wind variability. *Estuarine, Coastal and Shelf Science,* 61(2), 261–273.

Simionato, C. G., Meccia, V. L., Dragani, W. C., Guerrero, R. & Nuñez M. N. 2006. Rıo de la Plata estuary response to wind variability in synoptic to intraseasonal scales: Barotropic response. *Journal of Geophysical Research: Oceans,* 111(C9). DOI: https://doi.org/10.1029/2005JC003297

Stoddard, I., Anderson, K., Capstick, S., Carton, W., Depledge, J., Facer, K., Gough, C., Hache, F., Hoolohan, C., Hultman, M., Hällström, N., Kartha, S., Klinsky, S., Kuchler, M., Lövbrand, E., Nasiritousi, N., Newell, P., Peters, G. P., Sokona, Y. Stirling, A., Stilwell, M., Spash, C. L. & Williams, M. 2021. Three decades of climate mitigation: why haven't we bent the global emissions curve? *Annual Review of Environment and Resources*, 46(1), 653-689. DOI: https://doi.org/10.1146/annurev-environ-012220-011104

Vitousek, S., Barnard, P. L., Fletcher, C. H., Frazer, N., Eroksom, L. & Storlazzi C. D. 2017. Doubling of coastal flooding frequency within decades due to sea-level rise. *Scientific Reports,* 7, 1399. DOI: https://doi.org/10.1038/s41598-017-01362-7

Wood, M., Haigh, I. D., Quan Quan, L., Hung, N. N., Hoang T. B., Darby, S. E., Marsh, R., Skliris, N., Hirschi, J. J., Nicholls, R. J. & Bloemendaal, N. 2022. Climate-induced storminess forces major increases in future storm surge hazard in the South China Sea region*. Natural Hazards and Earth System Sciences,* 23(7), 2475-2504. DOI: https://doi.org/10.5194/nhess-23-2475-2023

Zhang, K., Li, Y., Liu, H., Xu, H., & Shen, J. 2013. Comparison of three methods for estimating the sea level rise effect on storm surge flooding. *Climatic Change*, 118(2), 487-500.